Statistical Theory of Deformed Nuclei*

K. A. Brueckner, R. C. Clark,† Wing-fai Lin, and R. J. Lombard‡
Institute for Pure and Applied Physical Sciences and Department of Physics, University of California at San Diego, La Jolla, California 92037

(Received 8 August 1969)

The changes in binding energy of $_{114}X^{298}$ under deformation into prolate spheroidal shapes have been calculated using the statistical theory of nuclei. The density is restricted only by the requirement that each equidense surface is a spheroid. It is found that the energy is minimized when the density has an approximately uniform surface thickness around the nucleus. To first order the change in binding energy is given well by the liquid-drop model, but at large deformation the statistical theory predicts less drop in energy and, consequently, a slightly more stable nucleus.

I. INTRODUCTION

THE statistical theory of nuclei has been successfully applied to the known nuclei by Brueckner *et al.*[1,2] In those papers, it was shown that the saturation curves of nuclear matter with variable neutron excess, as derived by Brueckner, Coon, and Dabrowski,[3] needed only minor adjustments to enable the statistical theory to reproduce the liquid-drop part of the binding energies of nuclei over a wide range of nucleon number. The confidence thus engendered in the statistical theory and in the energy functional used permits us to apply the method to study other macroscopic properties of nuclei and, in particular, to make predictions about the change in binding energy with deformation of the nucleus. The energy functional is sufficiently different from the Myers-Swiatecki mass formula[4] that even to obtain agreement with the predictions of that approach would in itself be interesting. One might expect, because of the additional degree of freedom (the changing denisty distribution), that the binding energy would be very different at any given quadrupole moment from that predicted by the mass formula. However, it must be remembered that the available parameters in the energy functional have been selected to reproduce the same binding energies as given by the mass formula for a large range of relative values of surface, Coulomb, and volume energies. Thus, a change in the relative values of these quantities (induced by a small deformation) may not result in a significant difference between the results obtained with the two approaches. On the other hand, there are correction terms inherent in the statistical theory (such as curvature effects and compressibility) that are neglected in the mass formulas and it is possible that these change significantly with deformation. The statistical theory only gives results averaged over the shell structure. However, shell corrections may be included in a self-consistent manner.

In this paper, we look at the change in binding energy of $_{114}X^{298}$ with deformation. This nucleus was chosen because it was predicted to have high stability against spontaneous fission and because of the current interest in its properties.[5–8] The type of deformations we permit the nucleus to have are such that any equidense contour in the nucleus—i.e., the surface on which the density is constant—is always a prolate spheroid. The eccentricity of these spheroids is variable and is taken to be a continuous function of the distance of the spheroid from the center of the nucleus. This function essentially determines the angular distribution of the density, and, together with the radial density distribution, must be varied to minimize the energy.

To illustrate the method, let us first consider the case of all density contours having the same eccentricity ϵ. We can describe the density by its variation along the minor axis b alone and we can scale b so that the density could have been obtained by an incompressible deformation of a spherical distribution ρ_0. Writing $b=r_0(1-\epsilon^2)^{1/6}$ ensures that the volume of the spheroid is the same as the volume of a sphere of radius r_0 and $\rho(\mathbf{r})=\rho_0(r_0)$. We split $E[\rho]$ [see (5) below] into three parts: $E_{\rm vol}[\rho]$ which contains all terms dependent on powers of ρ, including the Coulomb exchange energy, $E_{\rm grad}[\rho]$ containing terms dependent on the gradient of ρ, and $E_{\rm Coul}[\rho]$, the direct Coulomb energy. Expressing each term as an integral over $\mathbf{r}_0$ instead of $\mathbf{r}$ we have, for all n,

$$\int \rho^n(\mathbf{r})\,d^3r=\int \rho_0{}^n(r_0)\,d^3r_0,$$

so that

$$E_{\rm vol}[\rho(\mathbf{r})]=E_{\rm vol}[\rho_0(r_0)];$$

$$\int(\nabla\rho)^2 d^3r=f(\epsilon)\int(\partial\rho_0/\partial r_0)^2 d^3r_0,$$

* Research supported by the U.S. Atomic Energy Commission under Contract No. AT(11-1)-GEN-10, P.A. 11: Report No. UCSD 10P11-96.

† Present address: Department of Natural Philosophy, University of Aberdeen, Aberdeen, Scotland.

‡ Present address: Institut de Physique Nucléaire, Division de Physique Théorique, Laboratoire associé au CNRS, 91-Orsay, France.

[1] K. A. Brueckner, J. R. Buchler, S. Jorna, and R. J. Lombard, Phys. Rev. **171**, 1188 (1968).

[2] K. A. Brueckner, J. R. Buchler, R. C. Clark, and R. J. Lombard Phys. Rev. **181**, 1543 (1969).

[3] K. A. Brueckner, S. A. Coon, and J. Dabrowski, Phys. Rev. **168**, 1184 (1968).

[4] W. D. Myers and W. J. Swiatecki, Nucl. Phys. **81**, 1 (1966); Arkiv Fysik **36**, 343 (1967).

[5] S. G. Nilsson, J. R. Nix, A. Sobiczewski, Z. Szymánski, S. Wycech, C. Gustafson, and P. Möller, Nucl. Phys. **A115**, 545 (1968).

[6] G. T. Seaborg and J. L. Bloom, Sci. Am. **220**, 57 (1968).

[7] S. G. Nilsson, S. G. Thompson, and C. F. Tsang, Phys. Letters **28B**, 458 (1969).

[8] J. R. Nix, Report No. La-DC-10530, 1969 (unpublished).

where

$$f(\epsilon)=(1-\tfrac{1}{3}\epsilon^2)/(1-\epsilon^2)^{1/3},$$

so that

$$E_{\rm grad}[\rho(\mathbf{r})]=f(\epsilon)E_{\rm grad}[\rho_0(r_0)],$$

and

$$\int[\rho(\mathbf{r})\rho(\mathbf{r}')/|\mathbf{r}-\mathbf{r}'|]d^3r d^3r'=g(\epsilon)\times\int[\rho_0(r_0)\rho_0(r'_0)/|\mathbf{r}_0-\mathbf{r}'_0|]d^3r_0\,d^3r'_0, \quad (1)$$

where

$$g(\epsilon)=(1/2\epsilon)(1-\epsilon^2)^{1/3}\ln\{(1+\epsilon)/(1-\epsilon)\}.$$

The simple form of (1) (of which the usual liquid-drop form[9] is a special case) results from the fact that the equidense contours are similar concentric ellipsoidal shells[10] and that the potential is constant inside such a shell.

Hence, finally

$$E[\rho(\mathbf{r})]=E_0[\rho_0(r_0)]=E_{\rm vol}[\rho_0(r_0)]+f(\epsilon)E_{\rm grad}[\rho_0(r_0)]+g(\epsilon)E_{\rm Coul}[\rho_0(r_0)],$$

which is particularly easy to handle. As for the spherical case, we may readily derive the Euler-Lagrange equation to minimize $E_0[\rho_0]$ with respect to $\rho_0(r_0)$.

The intrinsic quadrupole moment of a deformed nucleus is

$$Q=(Z/A)\int\rho(\mathbf{r})(3z^2-r^2)d^3r. \quad (2)$$

For this density distribution it can also be expressed as an integral over r_0, namely,

$$Q=\frac{2\epsilon^2}{3(1-\epsilon^2)^{2/3}}4\pi\frac{Z}{A}\int_0^\infty\rho_0(r_0)r_0^4dr_0. \quad (3)$$

The above method cannot yield the best density distribution, as the angular dependence is too restricted. It is clear that the surface thickness, for example, is narrow on the minor and wide on the major axis of the nucleus. Physically, one would anticipate a more uniform surface thickness and this can be achieved by permitting the eccentricities of the spheroidal shells to be a function of b, the distance along the minor axis, especially in the surface region. The eccentricity function is found variationally, as will be described in Sec. III. Now the energy can no longer be split into simple factors as above, although the angular parts of some of the integrals may still be done. The most difficult term is the Coulomb energy which now becomes complicated but only weakly dependent on the additional density change. We can handle this by assuming that we may still factorize out the angular part as above and choose the factor self-consistently so the correct Coulomb contribution to the total energy is given. In other words, for each eccentricity function, we assume that the density and energy may be obtained by minimizing

$$E[\rho]=E_{\rm vol}[\rho_1,\epsilon]+E_{\rm grad}[\rho_1,\epsilon]+g_1(\epsilon)E_{\rm Coul}[\rho_1], \quad (4)$$

where ρ_1 is the density analogous to ρ_0 above. This process is recycled until self-consistency of $g_1(\epsilon)$ and ρ has been achieved. In Sec. II, we shall describe in greater detail how the energy functional may be brought to a form from which we can derive the associated Euler-Lagrange equation for the density distribution.

II. DIFFERENTIAL EQUATION

In Ref. 1, it was shown that the binding energies of the known nuclei could be obtained by minimizing

$$E[\rho]=\int\{C_K(\alpha)\rho^{5/3}+\rho V(\rho,\alpha)+\tfrac{1}{2}e[(1-\alpha)/2]\rho\phi_c-0.7836e^2[(1-\alpha)/2]^{4/3}\rho^{4/3}+(\hbar^2/8M)\eta[(\nabla\rho)^2+\theta(\nabla(\rho\alpha))^2]\}d^3r, \quad (5)$$

where $\rho=\rho_n+\rho_p$,

$$\alpha=(\rho_n-\rho_p)/\rho,\qquad \int\rho_n d^3r=N,\qquad \int\rho_p d^3r=Z,$$

$$C_K(\alpha)=\tfrac{3}{5}(\hbar^2/2M)(\tfrac{3}{2}\pi)^{2/3}\tfrac{1}{2}[(1-\alpha)^{5/3}+(1+\alpha)^{5/3}],$$

and

$$V(\rho,\alpha)=b_1(1+a_1\alpha^2)\rho+b_2(1+a_2\alpha^2)\rho^{4/3}+b_3(1+a_3\alpha^2)\rho^{5/3}.$$

Here $V(\rho,\alpha)$ and η have the "improved" values given in Ref. 2.

For simplicity, we assume here that α is constant throughout the nucleus, i.e., $\alpha=(N-Z)/A$. This approximation for the known spherical nuclei tends to give too small a binding energy per particle for nuclei with large α. However, here we are not comparing nuclei with different α and we are only looking at changes in energy and not at precise totals. Relaxing the proportionality between the densities might result in different deformations of ρ_n and ρ_p, thereby increasing the rate of decrease of the energy with deformation.

Instead of having a completely general spatial distribution restricted only by the total particle number condition, we simplify the angular dependence of the deformed density by assuming that all equidense surfaces are prolate spheroids with eccentricities $\epsilon(b)$ dependent on the length b of their minor axes. We shall discuss this approximation later in Sec. III. This density can be described by its variation along the minor axis alone, $\rho(\mathbf{r})=\rho_1(r_0)$, where

$$r=b/[1-\epsilon^2(b)\cos^2\theta]^{1/2}. \quad (6)$$

By introducing the variable $\mathbf{r}_0$ defined by

$$r_0=b[1-\epsilon^2(b)]^{-1/6},\qquad \theta_0=\theta,\qquad \phi_0=\phi, \quad (7)$$

we can eliminate the dependence on $\epsilon(b)$ of terms like

[9] P. J. Siemens and H. A. Bethe, Phys. Rev. Letters 18, 704 (1967).

[10] B. C. Carlson, J. Math. Phys. 2, 441 (1961).

$\int\rho^n(\mathbf{r})d^3r$. That is,

$$\int\rho^n(\mathbf{r})d^3r=\int\rho_1{}^n(r_0)d^3r_0, \tag{8}$$

as may be seen by changing coordinates from r, θ, ϕ to r_0, θ_0, ϕ_0. It is clear that r_0 is the radius of the spherical shell that would have resulted if we had incompressibly deformed the original prolate spheroidal shell into a spherical one. This is the physical reason why (8) holds.

The gradient energy term may also be reduced by the same substitution:

$$\int(\nabla\rho)^2d^3r=\int(\partial\rho_1/\partial r_0)^2d^3r_0 \times\left[\frac{(1-\frac{1}{3}\zeta^2)}{(1-\epsilon^2)^{1/3}}\left(\frac{\epsilon^2}{\zeta^2}+\frac{\zeta^2-\epsilon^2}{2\zeta^3}\log\frac{1+\zeta}{1-\zeta}\right)\right], \tag{9}$$

where

$$\zeta^2=-[b\epsilon/(1-\epsilon^2)](d\epsilon/db).$$

The Coulomb energy cannot be expressed as an integral in $\mathbf{r}_0$ space unless $\epsilon(b)$ is a constant. Hence, let us write

$$\rho(\mathbf{r})=\rho_c(\mathbf{r})+\delta\rho(\mathbf{r}), \tag{10}$$

where $\rho_c(\mathbf{r})$ is a density distribution formed from constant eccentricity prolate spheroids and $\delta\rho(\mathbf{r})$ may be positive or negative. Then

$$E_{\text{Coul}}[\rho(\mathbf{r})]=E_{\text{Coul}}[\rho_c(\mathbf{r})] +(e^2Z^2/A^2)\int[\delta\rho(\mathbf{r})\rho_c(\mathbf{r}')/|\mathbf{r}-\mathbf{r}'|]d^3r\,d^3r' +(e^2Z^2/2A^2)\int[\delta\rho(\mathbf{r})\delta\rho(\mathbf{r}')/|\mathbf{r}-\mathbf{r}'|]d^3r\,d^3r'. \tag{11}$$

The first term can be evaluated as in (1). The second represents the energy of $\delta\rho(\mathbf{r})$ in the potential of an ellipsoidal charge distribution. This potential is known analytically so that the whole term may be expressed as a three-dimensional numerical integral. The final term is best evaluated by expanding $\delta\rho(\mathbf{r})$ in Legendre polynomials and using the well-known expansion formula for $1/|\mathbf{r}-\mathbf{r}'|$. Only even-order polynomials are needed. The necessary convergence is obtained with the maximum order of 14, in less than 30 sec of computation time on a CDC 3600. A comparison of numerical and analytical evaluations of $E_{\text{Coul}}[\rho_c(\mathbf{r})]$ shows that the accuracy of the numerical methods employed is excellent. Each of the last two terms is a small correction to the first term so we may take $\rho_1(r_0)$ as being equivalent to some $\rho_0(r_0)$ and include in the energy functional an expression of the form

$$E_{\text{Coul}}[\rho(\mathbf{r})]=D_{ec}(e^2Z^2/2A^2) \times\int[\rho_1(r_0)\rho_1(r'_0)/|\mathbf{r}_0-\mathbf{r}'_0|]d^3r_0d^3r'_0, \tag{12}$$

where D_{ec} is a constant that gives the correct total Coulomb energy when $\rho(\mathbf{r})$ is known. This approximation enables us to minimize $E[\rho]$ in the usual manner and may be checked by taking the output ρ and evaluating $E_{\text{Coul}}[\rho]$ again. Although the total energy is fairly sensitive to D_{ec} because of the large value of the Coulomb energy contribution, this contribution itself is not very sensitive to $\rho(\mathbf{r})$ and self-consistency of D_{ec} is easily obtained. We were able to test the approximation by making the same assumption for E_{grad}. We calculated the minimum energy using (9) and also by replacing the bracketed expression by a constant, chosen to give the same gradient energy. Despite the fact that the density should be much more sensitive to the weight function in E_{grad} than to that in E_{Coul}, neither it nor the total energy was altered by more than 0.001%.

Substituting (8), (9), and (12) into (5) gives us an energy functional in $\mathbf{r}_0$ space. From this the Euler-Lagrange differential equation may be derived as described in Ref. 1. It only differs from the spherical case by a function of r_0, the bracketed expression in (9) and the factor D_{ec} in front of the electrostatic term.

Finally, the quadrupole moment for this density distribution is

$$Q=4\pi\frac{Z}{A}\int_0^\infty\rho_1(r_0)r_0{}^4dr_0\,\frac{2}{3(1-\epsilon^2)^{2/3}}\,\frac{\epsilon^2-\frac{1}{5}\zeta^2(2+\epsilon^2)}{1-\frac{1}{3}\zeta^2}. \tag{13}$$

III. VARIATIONAL ECCENTRICITY FUNCTION

The function $\epsilon(b)$ is found variationally. We can get an estimate of the function we are looking for by assuming that the surface has the same thickness on both the major and minor axes. Then $\epsilon(b)$ would be given by

$$\epsilon(b)=[1-b^2/(b+\lambda)^2]^{1/2}, \tag{14}$$

where λ is a constant. Alternatively, we can require the eccentricity to have a given value $\epsilon_{\max}$ at the edge of the nucleus, i.e., at a known value of b, thus determining the value of λ. It is easier to predetermine the quadrupole moment this way. As a further variational parameter we may make $\epsilon(b)$ vary more or less rapidly than (14), still keeping the value $\epsilon_{\max}$ at the edge of the nucleus by writing

$$\epsilon(b)=[1-b^2/(b+\lambda)^2]^{1/2}(1+u)-u\epsilon_{\max}. \tag{15}$$

The values u can take are limited by the requirement that ϵ cannot exceed unity and also that no two ellipsoids can cross. Equation (15) is then used in the "surface region" of the nucleus but $\epsilon(b)$ may be taken as constant in the central region of the nucleus, where the density is nearly constant anyway. We thus have three variational parameters: $\epsilon_{\max}$ (or λ), the "surface region" thickness t, and u. These parameters are determined self-consistently with the density. In practice, the energy is only slowly varying around the optimum value of u and is very insensitive to t provided it is large enough, i.e., $t\gtrsim5.0$. Other possible forms of eccentricity function have been tried but gave higher energies. We also evaluated E_{grad} using a strictly uniform surface outside an ellipsoid. The difference

TABLE I. The changes in total energy, volume energy, gradient, and Coulomb energy with each deformation. Energies are given in MeV and the quadrupole moment in barns.

Type of deformation	Quadrupole moment	E_{tot}	E_{vol}	E_{grad}	E_{Coul}
Spherical		−2057.39	−3969.23	421.26	1490.08
(1)	14.15	+2.80	0	+10.97	−8.17
(2)	14.15	+1.86	+5.72	+5.27	−9.13
(3)	14.32	+0.11	+5.38	+4.35	−9.62
(1)	23.10	+6.10	0	+25.61	−19.31
(2)	23.10	+3.87	+13.40	+11.87	−21.40
(3)	22.80	−0.01	+11.91	+9.66	−21.58
(1)	41.28	+14.03	0	+62.72	−48.69
(2)	41.28	+7.40	+32.12	+28.66	−53.38
(3)	40.14	−1.47	+28.56	+22.92	−52.95
(1)	56.27	+21.24	0	+96.65	−75.41
(2)	56.27	+9.58	+48.35	+43.30	−82.07
(3)	54.98	−2.85	+43.80	+35.47	−82.12

between the value obtained and that found using (14) was negligible even at the largest deformation. Equation (15) gives lower total energy and is simpler to use.

It should be noted that the deformed density given by this method is not as general as might be wished. The density along both major and minor axes of the deformed nucleus has a similar profile. Thus if there is a bottleneck effect on the major axis, there is also one on the minor axis. The Coulomb energy, however, might be further reduced by piling up the density at the far ends of the nucleus but this effect cannot be reproduced by our density. A density distribution in which the density is higher at the ends than in the middle has some density contours that intersect certain radius vectors more than once. Although it is possible to write down relationships between r_0 and r, θ that generate families of curves of this type, they are not as easily handled as the curves used in this paper. The restricted density we have used will only be valid while the nucleus shows no trace of necking. More explicitly, our deformations are restricted to Nilsson's ϵ distortions[11]; we have no ϵ_4 contribution. In view of this, we have made a comparison with predictions from the Myers-Swiatecki mass formula, when only the same restricted form of density contours are allowed. This will be discussed in Sec. IV.

IV. RESULTS

The results are shown in Fig. 1 and in Table I. In Fig. 1, curves (1)–(3) show the changes in total binding energy with deformation, i.e., deformation energy, for three different types of deformation. Curve (1) corresponds to an incompressible deformation to ellipsoidal shape with no density redistribution. The spherical gradient energy is multiplied by $f(\epsilon)$ and the spherical Coulomb energy by $g(\epsilon)$, so curve (1) plots

$$[f(\epsilon)-1]E_{grad}+[g(\epsilon)-1]E_{Coul}.$$

There is no change in E_{vol} for an incompressible deformation.

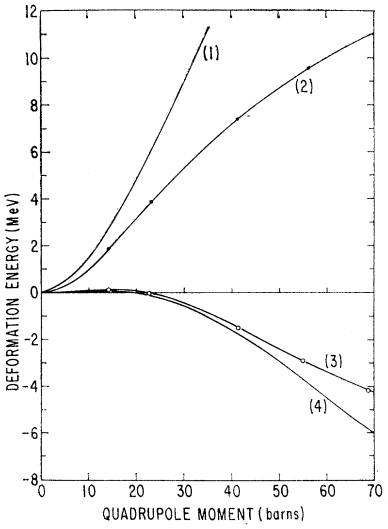

FIG. 1. The change in binding energy of $_{114}X^{298}$ plotted against quadrupole moment for three different types of deformation: (1) no radial redistribution of density and equidense surfaces restricted to be similar prolate spheroids, (2) with radial redistribution of density, and (3) equidense surfaces prolate spheroids of general eccentricity. Curve (4) is the Myers-Swiatecki (Ref. 4) liquid-drop model prediction for a prolate spheroidal deformation.

[11] S. G. Nilsson, Kgl. Danske Videnskab. Selskab, Mat.-Fys. Medd. 29, 1 (1955).

Curve (2) plots the deformation energy for the same type of deformation as in curve (1) but in addition allowing the radial density to redistribute itself to minimize the energy. This demonstrates the amount of reduction in energy that may be obtained by allowing $\rho(r)$ to freely minimize $E[\rho]$.

Curves (1) and (2) rise sharply because the surface of the nucleus has been deformed in such a way that it is stretched along the major axis and contracted along the minor axis. Curve (3) is obtained by allowing the eccentricity of the ellipsoidal contours to vary in such a was as to minimize this effect. It is clear from the figure that the minimum energy of a deformed nucleus will not be obtained unless the surface thickness of the nucleus is permitted to be roughly uniform.

Curve (4) is the liquid-drop model results of Myers and Swiatecki, where the drop is assumed to be deformed into an spheroid. The close agreement between the curves (3) and (4) for small deformations is the result of adjusting the saturation curves[2] so that the binding energy per particle agrees closely with those predicted by the Myers-Swiatecki liquid-drop[4] formula. A small deformation is equivalent to a slightly different relative weighting of surface, volume, and electrostatic energies, as is a change of A or Z. At large deformations, however, corrections from the curvature of the surface and the nonuniformity of the charge start to be important and the two results cannot be expected to agree. It should be emphasized that the curve (4) in no way represents a variational limit to our results. The two approaches are entirely different and an agreement between them is only because the parameters in both formulas have been adjusted to fit the same initial data.

Table I breaks down the total energy changes into contributions from the various components. The numbers (1)–(3) correspond to those of Fig. 1 and the types of deformation described above. Comparison between (1) and (2) shows that redistributing the density radially allows the gradient energy to decrease at the expense of an almost exactly equal increase in the volume energy and that the major part of the total energy change comes from the change in Coulomb energy. (Here the exchange Coulomb energy has been included in E_{vol} instead of E_{Coul} because of its volume-dependent form. This is in contrast to the E_{Coul} given in Ref. 2.) Thus the surface energy, defined as

$$E_{\text{surf}}=(E_{\text{tot}}-E_{\text{Coul}}-AE_{\text{sat}})/A^{2/3}$$

with E_{sat} being the minimum in the saturation curve for ${}_{114}X^{298}$, hardly alters with a redistribution of the radial density at a given quadrupole moment. To minimize E_{surf} we have to allow the angular density distribution to alter as is done in (3). Table I shows that between (2) and (3) the main part of the total energy change comes from E_{grad} plus E_{vol} and that E_{Coul} decreases only slightly. Note that the quadrupole moments are not exactly equivalent in (2) and (3).

TABLE II. The variational parameters needed in the eccentricity function to minimize the energy. The last column gives Nilsson's (Ref. 11) parameter ϵ giving rise to the same intrinsic quadrupole moment.

Q	$\epsilon_{\max}$	$b_{\max}$	u	ϵ
14.32	0.6	8.293	−0.2	0.223
22.80	0.7	7.998	−0.2	0.341
40.14	0.805	7.566	−0.1	0.544
54.98	0.855	7.276	−0.1	0.681

The variational parameters used in $\epsilon(b)$ to obtain the results in (3) are shown in Table II. $b_{\max}$ corresponds approximately to the length of the minor axis of the deformed nucleus. The fact that u is negative means that the density has a slightly larger surface thickness on the major axis than on the minor axis. Also shown in the last column of Table II is the value of Nilsson's parameter[9] ϵ that would give the same quadrupole moment to a liquid-drop nucleus. To obtain this we use the fact that ϵ is exactly related to ω, the ratio of the major axis to the minor axis of an ellipsoidal nucleus, by

$$\omega=(3+\epsilon)/(3-2\epsilon)$$

and that Q, the quadrupole moment, is given by

$$Q=\tfrac{2}{5}[(\omega^2-1)/\omega^{2/3}]Z\langle r^2\rangle.$$

In the last column of Table II and in (4) of Fig. 1, we have taken $\langle r^2\rangle=0.6A^{2/3}r_0^2$, where $r_0=1.2249$ fm.[4]

V. CONCLUSION

We have shown that the energy-density formalism may be successfully used to study deformed nuclei as well as spherical ones. It has the advantage over liquid-drop models in that internal changes in the density distribution with deformation can be made, resulting in correct handling of energy changes. On the other hand the liquid-drop model is considerably simpler to use and gives very similar results. The confirmation that the Myers-Swiatecki mass formula may be extended beyond the known nuclei into the region of large deformations is an important outcome because it has been shown[12] that the predictions of mass formulas are very sensitive to the parameters used.

A number of improvements on the procedure used in this paper may be made. First, the proton and neutron densities should be able to deform independently. Second, the charge density should be allowed to pile up at the ends of the major axis instead of being symmetrically spread around the origin. Both these effects would act to drop the energy at large deformations ($Q\gtrsim 30$b).

The approximate agreement between our curve and

[12] Cheuk-Yin Wong, Phys. Rev. Letters **19**, 328 (1967).

that of Myers and Swiatecki means that if the difference between curves (3) and (4) is added to the fission barrier of Ref. 5, the change in lifetime is small. The prediction of 2×10^{19} yr there will become 2×10^{21} yr. Since most of this change comes from the strongly deformed part of the fission barrier, the improvements mentioned above can be expected to shorten this lifetime. For $_{114}X^{298}$ with its short α-particle decay lifetime, this may not be important, but for $_{110}X^{294}$ where the fission and α-particle decay lifetimes are close, the fission lifetime may determine the total lifetime.

Shell-effect corrections can be calculated self-consistently for our statistical energy surface, following Strutinsky's approach.[13] Shell-model potentials can be obtained directly from the deformed densities[14] derived here. This way we shall avoid the usual uncertainties in extrapolating phenomenological shell-model potentials and can make more reliable predictions of the variation of potential with deformation. A study of this program is presently being made.

[13] V. M. Strutinsky, Nucl. Phys. **A95**, 420 (1967); **A122**, 1 (1968).

[14] K. A. Brueckner, Wing-fai Lin, and R. J. Lombard, Phys. Rev. **181**, 1506 (1969).

PHYSICAL REVIEW C VOLUME 1, NUMBER 1 JANUARY 1970

Decays of Tm^{170} and Tm^{171}: L_2 and L_3 Subshell-Fluorescence Yields, Coster-Kronig Transition Probabilities, and K-Shell Conversion Coefficients in Yb†

S. MOHAN, H. U. FREUND, AND R. W. FINK
School of Chemistry, Georgia Institute of Technology, Atlanta, Georgia 30332
AND
P. VENUGOPALA RAO
Department of Physics, Emory University, Atlanta, Georgia

(Received 1 August 1969)

High-resolution Ge(Li) and Si(Li) x-ray detectors [404- and 290-eV full width at half-maximum (FWHM) at 6.4 keV, respectively] were employed to study the singles and coincidence spectra of x rays and γ rays from the decays of Tm^{170} and Tm^{171}. Measurements of the rates of L_α, L_β, and L_γ x-ray emission in coincidence with $K_{\alpha1}$ and $K_{\alpha2}$ x rays yielded the following values for L_2 and L_3 subshell-fluorescence yields (ω_2, ω_3), L_2-L_3X Coster-Kronig transition probability (f_{23}), and relative L x-ray intensity ratios (s_2, s_3): $\omega_2=0.182\pm0.011$, $\omega_3=0.183\pm0.011$, $f_{23}=0.170\pm0.009$, $s_2=0.192\pm0.010$, and $s_3=0.165\pm0.009$. The K-conversion coefficient of the 84.3-keV $E2$ transition in Yb^{170} is found to be 1.39 ± 0.04 by the measurement of the intensity ratio for the K-x-ray and γ transitions (XPG method). The K-conversion coefficient of the 66.7-keV transition in Yb^{171} is found to be 7.45 ± 0.36, which leads to a value of 0.34 for the mixing ratio of $E2/M1$. The orbital-electron-capture branchings of Tm^{170} to the first excited state (78.6 keV) and to the ground state in Er^{170} are determined to be 0.04 and 0.10%, respectively.

I. INTRODUCTION

THE present investigation was carried out particularly to exploit the new high-resolution techniques developed during recent years in low-energy photon spectrometry. Detectors of Si(Li) and Ge(Li) with sufficient resolution to separate clearly the full-energy peaks above $Z\approx65$ of the $K_{\alpha1}$, $K_{\alpha2}$, $K_{\beta1}'$, and $K_{\beta2}'$ components of K x rays and the L_l, L_α, L_β, and L_γ components of the L x rays of interest are available. Coincidence methods[1] are employed to measure the L_2 and L_3 subshell-fluorescence yields and the L_2-L_3X Coster-Kronig transition probability in Yb from decay of Tm^{170} and Tm^{171}. No prior measurements on Yb exist in which a radioactive source of L subshell vacancies is used. Jopson *et al.*[2] measured L_2 and L_3 subshell-fluorescence yields by coincidence methods with NaI(Tl) detection and Yb foil targets in which K and L ionization was produced by an incident beam of γ rays from a Co^{57} source.

The K-shell conversion coefficient of the 84.3-keV $E2$ transition in Yb^{170} following the β decay of Tm^{170} has been of considerable interest and has been the subject of many investigations since 1952. This transition was one of the first leading to a suspicion at one time that anomalies existed in experimental $E2$ conversion coefficients in the deformed region. Essentially three different techniques were employed to measure α_K: (1) Measurement of the intensity ratio of the K-x-ray

* Work supported in part by the U.S. Atomic Energy Commission at Georgia Tech.

[1] P. Venugopala Rao, R. E. Wood, J. M. Palms, and R. W. Fink, Phys. Rev. **178**, 1997 (1969).

[2] R. C. Jopson, J. M. Khan, Hans Mark, C. D. Swift, and M. A. Williamson, Phys. Rev. **133**, A381 (1964).